Quantum Behavior of Space Debris and its Double-Slit Simulation due to Ultimate Acceleration

Huaiyang Cui
Department of Physics, Beihang University, Beijing, 100191, China
Email: hycui@buaa.edu.cn , hycui.blogspot.com
(July 14, 2022)

Abstract: In analogy with the ultimate speed c, there is an ultimate acceleration β, nobody's acceleration can exceed this limit β, in the solar system, β=2.961520e+10(m/s^2). Because this ultimate acceleration is a large number, any effect connecting to β will become easy to test, including quantum gravity tests. In this paper, an approach is put forward to connect the ultimate acceleration with quantum theory, as an application, the quantum theory with the ultimate acceleration provides a useful formula to calculate the space debris distribution around the earth, this calculation results agree well with the experimental observation which are a set of measurements by incoherent scattering radar of EISCAT in the Arctic circle. Using the same approach, the radius of the Sun is calculated out to be r=7e+8 (m) with a relative error 0.72%; the radius of the Earth is calculated out to be r=6.4328e+6 (m) with a relative error 0.97%. The double-slit interference of space debris is also investigated for demonstrating its quantum behavior.

1. Introduction

In analogy with the ultimate speed c, there is an ultimate acceleration β, nobody's acceleration can exceed this limit β, in the solar system, β=2.961520e+10(m/s^2). Because this ultimate acceleration is a large number, any effect connecting to β will become easy to test, including quantum gravity tests. In this paper, an approach is put forward to connect the ultimate acceleration with quantum theory, as an application, the quantum theory with the ultimate acceleration provides a useful formula to calculate the space debris distribution around the earth, this calculation results agree well with the experimental observation which are a set of measurements by incoherent scattering radar of EISCAT in the Arctic circle. The double-slit interference of space debris is also investigated for demonstrating its quantum behavior.

With the increasing frequency of human space activities, the impact and harm of space debris are becoming more and more obvious [16,17]. The monitoring and early warning of space debris have gradually been widely investigated [18,19,20]. The Arctic is a key area for space debris monitoring. At present, incoherent scattering radar is the most powerful ground-based ionospheric monitoring means in the world. It mainly studies the ionospheric space environment information by receiving the backscattered echo of transmitted wave. Since the 1960s, more than 10 sets of incoherent scattering radars have been built, mainly by the American and European incoherent scattering radar Scientific Association (EISCAT). The observational data source used in this paper is a set of measurements by incoherent scattering radar of EISCAT in the Arctic circle (i.e. ESR radar) [21-25].

2. How to connect quantum theory with ultimate acceleration

In the relativity, the speed of light c is an ultimate speed, nobody's speed can exceed this limit c. The relativistic velocity u of a particle in the coordinate system ($x_1,x_2,x_3,x_4=ict$) satisfies

$$u_1^2+u_2^2+u_3^2+u_4^2=-c^2 \quad . \tag{1}$$

No matter what particles (electrons, molecules, neutrons, quarks), their 4-vector velocities all have the same magnitude: $|u|=ic$. All particles gain **equality** because of the same magnitude of their 4-velocity u. The acceleration a of the particle is given by

$$a_1^2+a_2^2+a_3^2=a^2; \quad (a_4=0; \quad \because x_4=ict) \tag{2}$$

Assume that particles have an ultimate acceleration β as limit, no particle can exceed this acceleration limit β. Subtracting the both sides of the above equation by β^2, we have

$$a_1^2+a_2^2+a_3^2-\beta^2=a^2-\beta^2; \qquad a_4=0 \tag{3}$$

It can be rewritten as

$$[a_1{}^2+a_2{}^2+a_3{}^2+0+(i\beta)^2]\frac{1}{1-a^2/\beta^2}=-\beta^2 \tag{4}$$

Now, the particle subjects to an acceleration whose five components are specified by

$$\begin{aligned}
&\alpha_1=\frac{a_1}{\sqrt{1-a^2/\beta^2}}; \quad \alpha_2=\frac{a_2}{\sqrt{1-a^2/\beta^2}}; \\
&\alpha_3=\frac{a_3}{\sqrt{1-a^2/\beta^2}}; \quad \alpha_4=0; \quad \alpha_5=\frac{i\beta}{\sqrt{1-a^2/\beta^2}};
\end{aligned} \tag{5}$$

where α_5 is the newly defined acceleration in five dimensional space-time ($x_1,x_2,x_3,x_4=ict,x_5$). Thus, we have

$$\alpha_1^2+\alpha_2^2+\alpha_3^2+\alpha_4^2+\alpha_5^2=-\beta^2; \quad \alpha_4=0 \tag{6}$$

It means that the magnitude of the newly defined acceleration α for every particle takes the same value: $|\alpha|=i\beta$ (constant imaginary number).

How to resolve the velocity u and acceleration α into x, y and z components? In realistic world, a hand can rotate a ball moving around a circular path at constant speed v with constant centripetal acceleration a, as shown in Fig.1(a).

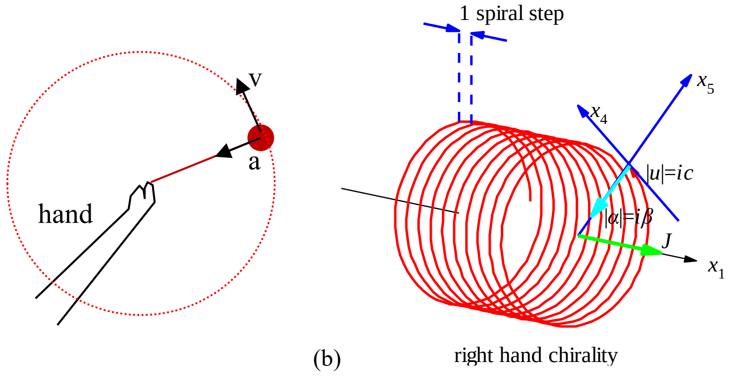

Fig.1 (a) A hand rotates a ball moving around a circular path at constant speed v with constant centripetal acceleration a. (b) The particle moves along the x_1 axis with the constant speed $|u|=ic$ in the u direction and constant centripetal force in the x_5 axis at the radius iR (imaginary number).

```
<Clet2020 Script>//Clet v3 is a free C compiler[26]
double D[100],S[2000];int i,j,R,X,N;
int main(){R=50;X=50;N=600;D[0]=-50;D[1]=0;D[2]=0;D[3]=X;D[4]=0;D[5]=0;D[6]=-50;D[7]=R;D[8]=0;
D[9]=600;D[10]=10;D[11]=R;D[12]=0;D[13]=3645;
Lattice(SPIRAL,D,S);SetViewAngle(0,80,-50);DrawFrame(FRAME_NULL,1,0xffffff);
Draw("LINE,0,2,XYZ,0","-150,0,0,-50,0,0");Draw("ARROW,0,2,XYZ,10","50,0,0,150,0,0");
SetPen(2,0xff0000);Plot("POLYLINE,0,600,XYZ",S[9]);i=9+3*N-6;Draw("ARROW,0,2,XYZ,10",S[i]);
TextHang(S[i],S[i+1],S[i+2],"   #if|u|=ic#t");TextHang(150,0,0,"   #ifx#sd1#t");SetPen(2,0x005fff);
Draw("LINE,1,2,XYZ,8","-50,0,50,-50,0,100");Draw("LINE,1,2,XYZ,8","-40,0,50,-40,0,100");
Draw("ARROW,0,2,XYZ,10","-80,0,100,-50,0,100");Draw("ARROW,0,2,XYZ,10","-10,0,100,-40,0,100");
TextHang(-50,0,110,"1 spiral step");i=9+3*N;S[i]=50;S[i+1]=10;S[i+2]=10;
Draw("ARROW,0,2,XYZ,10","50,0,0,50,80,80");TextHang(50,80,80," #ifx#sd5#t");
Draw("ARROW,0,2,XYZ,10","50,72,0,50,0,72");TextHang(50,0,72,"   #ifx#sd4#t");
SetPen(3,0x00ffff);Draw("ARROW,0,2,XYZ,15",S[i-3]);TextHang(S[i],S[i+1],S[i+2],"   #if|α|=iβ#t");
SetPen(3,0x00ff00);Draw("ARROW,0,2,XYZ,15","50,0,0,120,0,0");TextHang(110,5,5," #ifJ#t");
TextHang(-60,0,-80," right hand chirality");}#v07=?>A
```

In analogy with the ball in a circular path, consider a particle in one dimensional motion along the x_1 axis at the speed v, in the Fig.1(b) it moves with the constant speed $|u|=ic$ almost along the x_4 axis and slightly along the x_1 axis, and the constant centripetal acceleration $|\alpha|=i\beta$ in the x_5 axis at the constant radius iR (imaginary number); the coordinate system ($x_1,x_4=ict,x_5=iR$) establishes a cylinder coordinate system in which this particle moves spirally at the speed v along the x_1 axis. According to usual centripetal acceleration formula $a=v^2/r$, the acceleration in the x_4-x_5 plane is given by

$$a=\frac{v^2}{r} \quad \Rightarrow \quad i\beta=\frac{|u|^2}{iR}=-\frac{c^2}{iR}=i\frac{c^2}{R} \quad . \tag{7}$$

Therefore, the track of the particle in the cylinder coordinate system ($x_1,x_4=ict,x_5=iR$) forms a shape, called as **acceleration-roll**. The faster the particle moves, the longer the spiral step is.

As like a steel spring that contains elastic wave, the track in the acceleration-roll in Fig.1(b) can be described by a wave function whose phase changes 2π for one spiral step. Apparently, this wave should be the de Broglie's matter wave for electrons, protons or quarks, etc.

Proof: The wave function phase changes 2π for one spiral circumferences $2\pi(iR)$, then a small displacement of the particle on the spiral track is $|u|d\tau=icd\tau$ in the 4-vector u direction, thus this wave phase along the spiral track is evaluated by

$$phase=\int_0^{\tau}\frac{2\pi}{2\pi(iR)}icd\tau=\int_0^{\tau}\frac{c}{R}d\tau \quad . \tag{8}$$

Substituting the radius R into it, the wave function ψ is given by

$$\psi=\exp(-i\cdot phase)=\exp(-i\int_0^{\tau}\frac{c}{R}d\tau)=\exp(-i\frac{\beta}{c}\int_0^{\tau}d\tau) \quad . \tag{9}$$

In the theory of relativity, we known that the integral along $d\tau$ needs to transform into realistic line integral, that is

$$\begin{aligned} d\tau &=-c^2\frac{d\tau}{-c^2}=(u_1^2+u_2^2+u_3^2+u_4^2)\frac{d\tau}{-c^2} \\ &=(u_1dx_1+u_2dx_2+u_3dx_3+u_4dx_4)\frac{1}{-c^2} \end{aligned} \quad . \tag{10}$$

Therefore, the wave function ψ is evaluated by

$$
\begin{aligned}
\psi &= \exp(-i\frac{\beta}{c}\int_0^{\tau} d\tau) \\
&= \exp(i\frac{\beta}{c^3}\int_0^{x}(u_1dx_1 + u_2dx_2 + u_3dx_3 + u_4dx_4))
\end{aligned} \quad . \tag{11}
$$

This wave function may have different explanations, depending on the particle under investigation. If the β is replaced by the Planck constant, the wave function of electrons is given by

$$
\begin{aligned}
&assume: \quad \beta = \frac{mc^3}{\hbar} \\
&\psi = \exp(\frac{i}{\hbar}\int_0^{x}(mu_1dx_1 + mu_2dx_2 + mu_3dx_3 + mu_4dx_4))
\end{aligned} \quad . \tag{12}
$$

where $mu_4dx_4=-Edt$, it strongly suggests that the wave function is just the de Broglie's matter wave [4,5,6].

In Fig.1(b), the acceleration-roll of particle moves with two distinctions: right-hand chirality and left-hand chirality. The direction of the angular momentum J would be slightly different from the x_1 due to spiral precession. It is easy to calculate the ultimate acceleration β , the radius R and the angular momentum J in the plane x_4-x_5 for spiraling electron as

$$
\begin{aligned}
&\beta = \frac{c^3 m}{\hbar} = 2.327421\text{e+29 (M/s}^2) \\
&R = \frac{c^2}{\beta} = 3.861593\text{e-13 (M)} \\
&J = \pm m\,|\,u\,|\,iR = \mp\hbar
\end{aligned} \quad . \tag{13}
$$

```
<Clet2020 Script>//Clet v3 is a free C compiler[26]
double beta,R,J,m,D[10];char str[200];
int main(){m=ME;beta=SPEEDC*SPEEDC*SPEEDC*m/PLANCKBAR;
R=SPEEDC*SPEEDC/beta;J=PLANCKBAR;Format(str,"beta=%e, #nR=%e, #nJ=%e",beta,R,J);
TextAt(50,50,str);ClipJob(APPEND,str);}#v07=#t
```

Considering another explanation to ψ for planets in the solar system, no Planck constant can be involved. But, in a many-body system with the total mass M, data-analysis (in the next section) tells us that the ultimate acceleration can be rewritten in terms of **Planck-constant-like constant** h as

$$
\begin{aligned}
&assume: \quad \beta = \frac{c^3}{hM} \\
&\psi = \exp(\frac{i}{hM}\int_0^{x}(u_1dx_1 + u_2dx_2 + u_3dx_3 + u_4dx_4))
\end{aligned} \quad . \tag{14}
$$

The constant h will be determined by experimental observations. In next section we shall try to use this wave function as the planetary scale waves in the solar system to explain quantum gravity effects for the planets and satellites, the wave function is called as the **acceleration-roll wave**.

Tip: actually, ones cannot get to see the acceleration-roll of particle in the relativistic space-time ($x_1,x_2,x_3,x_4=ict$) ; only get to see it in the cylinder coordinate system ($x_1,x_4=ict,x_5=iR$).[28]

3. The acceleration-roll wave in planetary systems

In the Bohr's orbit model for planets or satellites, as shown in Fig.2, the circular quantization condition is in terms of acceleration-roll wave given by

$$\left.\begin{aligned}\frac{\beta}{c^3}\oint_L v_l dl = 2\pi n\\ v_l = \sqrt{\frac{GM}{r}}\end{aligned}\right\} \Rightarrow \sqrt{r} = \frac{c^3}{\beta\sqrt{GM}}n; \quad n = 0,1,2,\dots \tag{15}$$

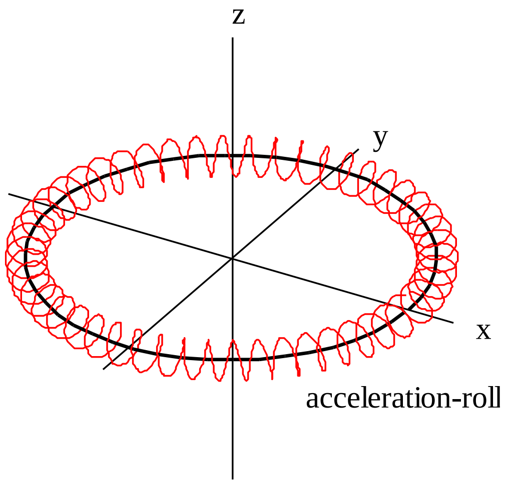

Fig.2 A planet 2D orbit around the sun, an acceleration-roll winding around the planet.

```
<Clet2020 Script>//Clet v3 is a free C compiler[26]
int i,j,k; double r,rot,x,y,z,D[20],F[20],S[200];
int main(){SetViewAngle("temp0,theta60,phi-30");
DrawFrame(FRAME_LINE,1,0xafffaf);r=80;Spiral(); TextHang(r,-r,0,"acceleration-roll");
r=110;TextHang(r,0,0,"x");TextHang(0,r,0,"y");TextHang(0,0,r,"z");}
Spiral(){r=80;j=10;rot=j/r;k=2*PI/rot+1;
for(i=0;i<k;i+=1) {D[0]=x;D[1]=y;D[2]=z;D[6]=x;D[7]=y;D[8]=r;
x=r*cos(rot*i);y=r*sin(rot*i);z=0;if(i==0) continue;
SetPen(2,0x00);F[0]=D[0];F[1]=D[1];F[2]=x;F[3]=y;Draw("LINE,0,2,XY,",F);SetPen(1,0xff0000);
D[3]=x;D[4]=y;D[5]=z; D[9]=40;D[10]=10;D[11]=8;D[12]=0;D[13]=360;
Lattice(SPIRAL,D,S);Plot("POLYLINE,0,40,XYZ",S[9]);}
}#v07=?>A
```

The solar system, Jupiter's satellites, Saturn's satellites, Uranus' satellites, Neptune's satellites as five different many-body systems are investigated with the Bohr's orbit model. After fitting observational data as shown in Fig.3, their ultimate accelerations are obtained in Table 1. The predicted quantization-blue-lines in Fig.3(a), Fig.3(b), Fig.3(c), Fig.3(d) and Fig.3(e) agree well with experimental observations for those *inner constituent planets or satellites*.

Besides every β, our interest shifts to the constant h in Table 1, which is defined as

$$h = \frac{c^3}{M\beta} \quad \Rightarrow \quad \sqrt{r} = h\sqrt{\frac{M}{G}}n \ . \tag{16}$$

In a many-body system with the total mass M, a constituent particle has the mass m and moves at the speed v, it is easy to find that the wavelength of de Broglie's matter wave should be modified for planets and satellites as

$$\lambda = \frac{2\pi\hbar}{mv} \quad \Rightarrow \text{modify} \Rightarrow \quad \lambda = \frac{2\pi hM}{v} \ . \tag{17}$$

where h is a **Planck-constant-like constant**. Usually the total mass M is approximately equal to the central-star's mass. It is found that this modified matter wave works for quantizing orbits correctly in Fig.3 [28,29]. The key point is that the various systems have almost same Planck-constant-like constant h in Table 1 with a mean value of 3.51e-16 $m^2s^{-1}kg^{-1}$, at least have the same magnitude! The acceleration-roll wave is a generalized matter wave as a planetary scale wave.

Table 1 Planck-constant-like constant h in various systems, N is constituent particle number with smaller inclination.

system	N	M/M_{earth}	β (m/s^2)	h (m^{2}s^{-1}kg^{-1})	Prediction
Solar planets	9	333000	2.961520e+10	4.574635e-16	Fig.3(a)
Jupiter' satellites	7	318	4.016793e+13	3.531903e-16	Fig.3(b)
Saturn's satellites	7	95	7.183397e+13	6.610920e-16	Fig.3(c)
Uranus' satellites	18	14.5	1.985382e+15	1.567124e-16	Fig.3(d)
Neptune 's satellites	7	17	2.077868e+15	1.277170e-16	Fig.3(e)

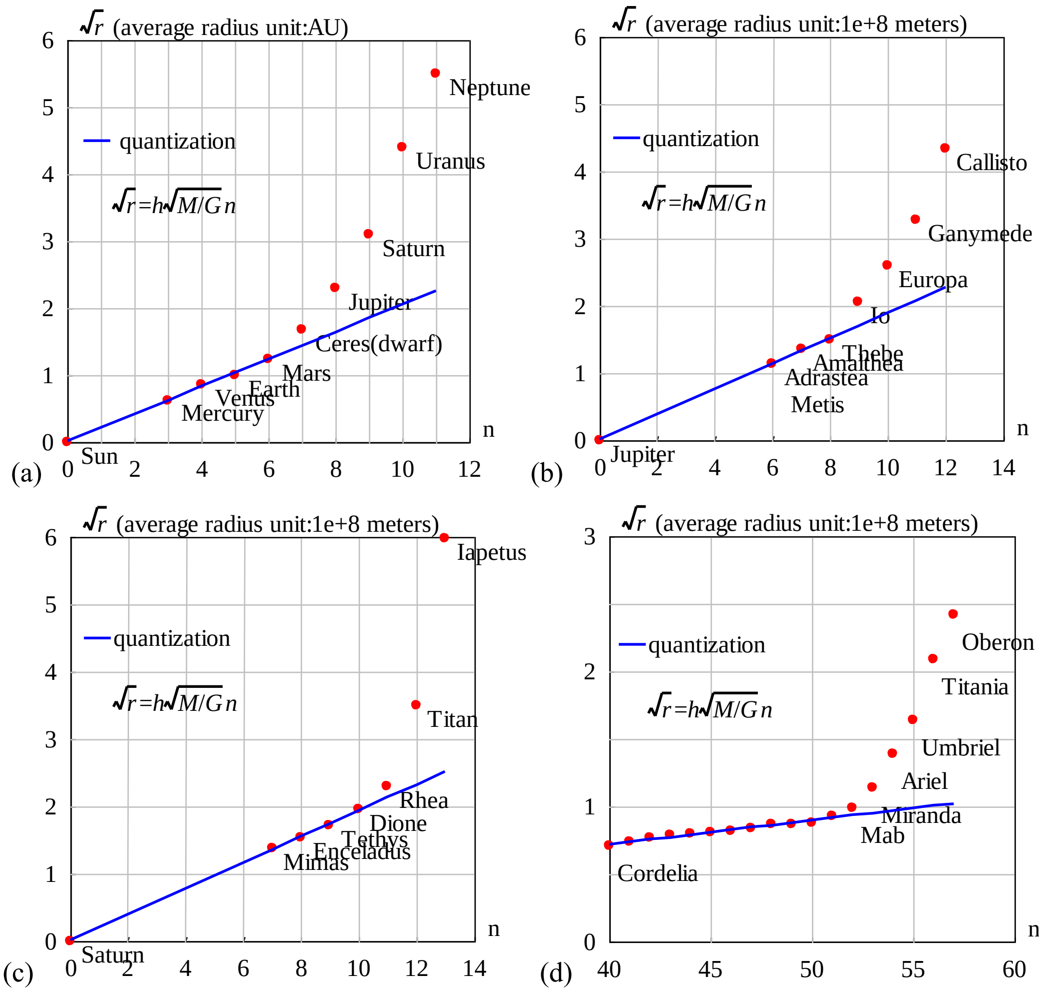

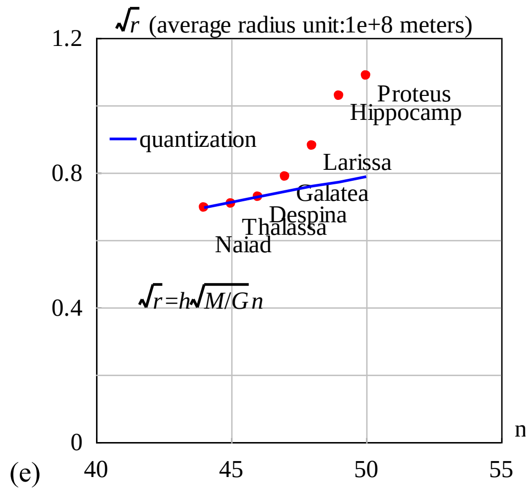

Fig.3 The orbital radii are quantized for inner constituents. (a) the solar system with h=4.574635e-16 ($m^2s^{-1}kg^{-1}$). The relative error is less than 3.9%. (b) the Jupiter system with h=3.531903e-16 ($m^2s^{-1}kg^{-1}$). Metis and Adrastea are assigned the same quantum number for their almost same radius. The relative error is less than 1.9%. (c) the Saturn system with h=6.610920e-16 ($m^2s^{-1}kg^{-1}$). The relative error is less than 1.1%. (d) the Uranus system with h=1.567124e-16 ($m^2s^{-1}kg^{-1}$). n=0 is assigned to the Uranus. The relative error is less than 2.5%. (e) the Neptune system with h=1.277170e-16 ($m^2s^{-1}kg^{-1}$). n=0 is assigned to the Neptune. The relative error is less than 0.17%.

In Fig.3(a), the blue straight line expresses the linear regression relation among the Sun, Mercury, Venus, Earth and Mars, their quantization parameters are hM=9.098031e+14(m^2/s). The ultimate acceleration is β=2.961520e+10 (m/s^2). Where, n=3,4,5,.. were assigned to solar planets, the sun was assigned a quantum number n=0 because the sun is in the **central state**.

4. Optical model of solar central state

The acceleration-roll wave as the generalized matter wave is given by

$$\psi = \exp(\frac{i}{hM}\int_0^x v_l dl); \quad \lambda = \frac{2\pi hM}{v_l} \quad . \tag{18}$$

In a central state n=0, if the coherent length of the acceleration-roll wave is long enough, its head may overlap with its tail when the particle moves in a closed orbit in the space time, as shown in Fig.4, the interference of the acceleration-roll wave between its head and tail will occur in the overlapping zone. Because the acceleration-roll wave winds around the time axis and overlaps itself, the overlapped wave is given by

$$\begin{aligned} \psi(r) &= 1 + e^{i\delta} + e^{i2\delta} + \ldots + e^{i(N-1)\delta} = \frac{1-\exp(iN\delta)}{1-\exp(i\delta)} \\ \delta(r) &= \frac{1}{hM}\oint_L (v_l)dl = \frac{2\pi\omega r^2}{hM} \end{aligned} \quad . \tag{19}$$

where N is the overlapping number which is determined by the coherent length of the acceleration-roll wave, δ is the phase difference after one orbital motion, ω is the angular speed of the sun rotation. The above equation is a multi-slit interference formula in optics, for a larger N it is called as the

Fabry-Perot interference formula.

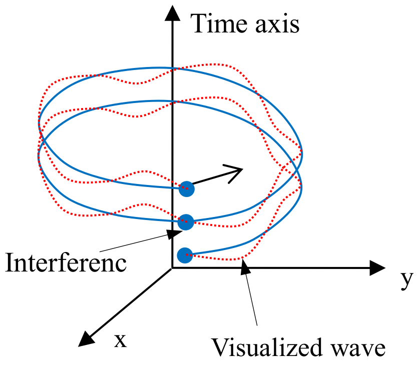

Fig.4 The head of the acceleration-roll wave may overlap with its tail.

The acceleration-roll wave function ψ needs a further explanation. In quantum mechanics, $|\psi|^2$ equals to the probability of finding an electron due to Max Burn's explanation; in astrophysics, $|\psi|^2$ equals to the probability of finding a nucleon (proton or neutron) *averagely in astronomic scale*, because all mass is mainly made of nucleons, we have

$$|\psi|^2 \propto nucleon\_density \quad . \tag{20}$$

It follows from the multi-slit interference formula that the interference intensity at maxima is proportional to N^2, that is

$$N^2 = \frac{|\psi(0)_{multi-wavelet}|^2}{|\psi(0)_{one-wavelet}|^2} \quad . \tag{21}$$

What matter plays the role of "one-wavelet" in the solar core or Earth core? We choose vapor above the sea on the earth surface as the "reference matter: one-wavelet". Thus, the overlapping number N is estimated by

$$N^2 = \frac{|\psi(0)_{multi-wavelet}|^2}{|\psi(0)_{one-wavelet}|^2} \approx \frac{core\_nucleon\_density_{r=0}}{vapor\_above\_sea\_density} \quad . \tag{22}$$

Although today there is not vapor on the solar surface, the solar core has a density of 1.5e+5kg/m^3 [31], comparing to the vapor density 1.29 kg/m^3 on the earth, the solar overlapping number N is estimated as N=341. The Earth core density is 5.53e+3kg/m^3, the Earth's overlapping number N is estimated as N=65.

For the Sun, Earth and Mars, their central densities and their reference matter density are given in the Table 2. Thus, their overlapping numbers are obtained also in this table.

Table 2 Estimating the overlapping number N by comparing solid core and reference matter, regarding protons and neutrons as basis particles.

object	Solid core, density (kg/m^3)	Reference matter, density (kg/m^3)	Overlapping number N	β (m/s^2)
Sun	1.5e+5 (max.)	1.29 (vapor above the sea)	341	2.961520e+10
Earth	5530	1.29 (vapor above the sea)	65	1.377075e+14
Mars	3933.5	1.29 (vapor above the sea)	55	2.581555e+15
Jupiter	1326			4.016793e+13

Saturn	687			7.183397e+13
Uranus	1270			1.985382e+15
Neptune	1638			2.077868e+15
Alien-planet	5500	1.29(has water on the surface)	65	

Sun's rotation angular speed at the equator is known as ω=2π/(25.05*24*3600), unit s^{-1}. Its mass 1.9891e+30 (kg), radius 6.95e+8 (m), mean density 1408 (kg/m^3), the solar core has a maximum density of 1.5e+5kg/m^3 [31], the ultimate acceleration β=2.961520e+10 (m/s^2), the constant hM= 9.100745e+14 (m^2/s). According to the N=341, the matter distribution of the $|\psi|^2$ is calculated out in Fig.5, it agrees well with the general description of the sun's interior. The radius of the Sun is calculated out to be r=7e+8 (m) with a relative error 0.72% in the Fig.5, it indicates that the sun radius strongly depends on the sun self-rotation.

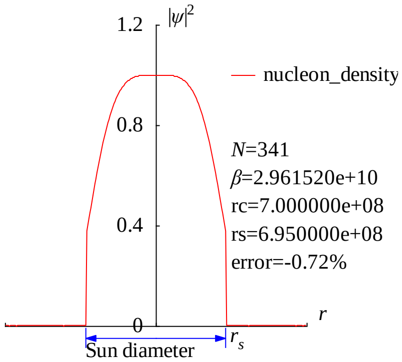

Fig.5 The matter distribution $|\psi|^2$ around the Sun has been calculated in radius direction.

```
<Clet2020 Script>//Clet v3 is a free C compiler[26]
int i,j,k,m,n,N,nP[10];
double beta,H,B,M,r,r_unit,x,y,z,delta,D[1000],S[1000], a,b,rs,rc,rot,atm_height; char str[100];
main(){k=150;rs=6.95e8;rc=0;x=25.05;rot=2*PI/(x*24*3600);n=0; N=341;
beta=2.961520e10;H=SPEEDC*SPEEDC*SPEEDC/beta;M=1.9891E30; atm_height=2e6; r_unit=1E7;
b=PI/(2*PI*rot*rs*rs/H);
for(i=-k;i<k;i+=1) {r=abs(i)*r_unit;
if(r<rs+atm_height) delta=2*PI*rot*r*r/H; else delta=2*PI*sqrt(GRAVITYC*M*r)/H;//around the star
y=SumJob("SLIT_ADD,@N,@delta",D); y=y/(N*N);
S[n]=i;S[n+1]=y; if(i>0 && rc==0 && y<0.001) rc=r;D[n]=i;D[n+1]=z;n+=2;}
SetAxis(X_AXIS,-k,0,k,"#ifr; ; ; ;");SetAxis(Y_AXIS,0,0,1.2,"#if|ψ|#su2#t;0;0.4;0.8;1.2;");
DrawFrame(FRAME_SCALE,1,0xafffaf); z=100*(rs-rc)/rs;
SetPen(1,0xff0000);Polyline(k+k,S,k/2,1," nucleon_density"); SetPen(1,0x0000ff); //Polyline(k+k,D);
//Draw("LINE,0,2,XY,0","20,0.5,60,0.6");TextHang(60,0.6,0,"core");
r=rs/r_unit;y=-0.05;D[0]=-r;D[1]=y;D[2]=r;D[3]=y; Draw("ARROW,3,2,XY,10,100,10,10,",D);
Format(str,"#ifN#t=%d#n#ifβ#t=%e#nrc=%e#nrs=%e#nerror=%.2f%",N,beta,rc,rs,z);
TextHang(k/2,0.7,0,str);TextHang(r+5,y/2,0,"#ifr#sds#t");TextHang(-r,y+y,0,"Sun diameter");
}#v07=?>A
```

5. Earth central state and space debris distribution

Appling the acceleration-roll wav to the Moon, as illustrated in Fig.6(a), the Moon has been assigned a quantum number of n=2 in author's early study [28]. According to Eq.(15), the ultimate acceleration is fitted out to be β=1.377075e+14 (m/s^2) in the Earth system. Another consideration is to take the quasi-satellite's perigee into account, for the moon and 2004_GU9 etc., as shown in Fig.6(b), but this consideration requires further understanding to its five quasi-satellites [28].

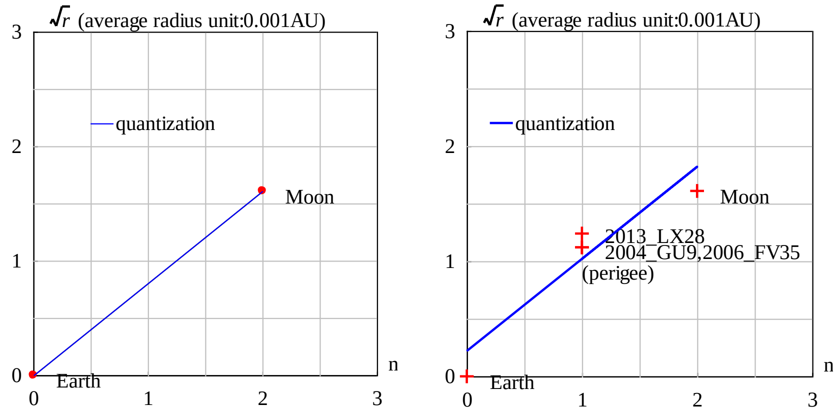

(a) H=1.956611e+11 B=0.000000e+00 (b) H=1.956611e+11 B=-5.221444e+10

Fig.6 orbital quantization for moon and quasi-satellites to the Earth, H=hM.

```
<Clet2020 Script>//Clet v3 is a free C compiler[26]
char str[200];int i,j,k,N,nP[10]; double x,y,z,M,r_unit,a,b,B,H,r_ave[20],dP[10],D[1000];
double orbit[10]={0,2.57,0,}; double e[10]={0, 0.0549,0,0,0,0,0,0,0,0,};
int qn[10]={0,2,3,4,5,6,7,8,9.,10,};
char Stars[100]={"Earth;Moon;"};
int main(){ N=2; M=5.97237E24; r_unit=1.495978707e8;
for(i=0;i<N;i+=1) {x=orbit[i];y=e[i]; z=x*(1+sqrt(1-y*y))/2;r_ave[i]=z;//average_radius
D[i+i]=qn[i];D[i+i+1]=sqrt(z); }
DataJob("REGRESSION,2",D,dP);b=dP[0];a=dP[1];
SetAxis(X_AXIS,0,0,3,"n;0;1;2;3;");
SetAxis(Y_AXIS,0,0,3," #if#rsr#t (average radius unit:0.001AU);0;1;2;3;");
DrawFrame(0x0166,1,0xafffaf); Polyline(N,D);
SetPen(2,0xff0000); Plot("OVALFILL,0,2,XY,3,3,",D);
for(i=0;i<N;i+=1) {nP[0]=TAKE;nP[1]=i;TextJob(nP,Stars,str);x=qn[i]+0.2;y=sqrt(orbit[i])-0.05;TextHang(x,y,0,str);}
x=GRAVITYC*M*r_unit;z=sqrt(x);H=z*a;B=-z*b;
TextAt(100,450,"#ifH#t=%e   #ifB#t=%e",H,B);
for(i=0;i<N;i+=1) {y=b+a*qn[i];D[i+i]=qn[i];D[i+i+1]=y;}
SetPen(1,0x0000ff);Polyline(N,D,0.5,2.2,"quantization");//check
}}#v07=?>A
```

Now let us talk about the central state of the earth n=0, the earth's rotation angular speed is known as ω=2π/(24*3600), unit s^{-1}. Its mass 5.97237e+24(kg), radius 6.371e+6(m), core density 5530(kg/m^3), the ultimate acceleration β=1.377075e+14(m/s^2), the constant hM=1.956611e+11(m^2/s).

We have estimated that the wave overlapping number in the central state of the earth is N=65, the matter distribution $|\psi|^2$ in radius direction is calculated out as shown in Fig.7(a), where the self-rotation near its equator has the period of 24 hours:

$$\delta(r) = \frac{1}{hM} \oint_L (v_l) dl = \frac{2\pi r}{hM} \omega r \quad . \tag{23}$$

There is a central maximum of matter distribution at the earth heart, which gradually decreases to zero near the earth surface, then rises the secondary peaks and attenuates down off. The radius of the earth is calculated out to be r=6.4328e+6 (m) with a relative error 0.97% using the interference of its acceleration-roll wave. Space debris over the atmosphere has a complicated evolution [7,8], has itself speed

$$v_l = \sqrt{\frac{GM}{r}}; \quad \delta(r) = \frac{1}{hM} \oint_L (v_l) dl = \frac{\beta}{c^3} \oint_L (v_l) dl = \frac{2\pi\beta}{c^3} \sqrt{GMr} \quad . \tag{24}$$

The secondary peaks over the atmosphere up to 2000km altitude is calculated out in Fig.7(b) which agrees well with the space debris observations [16]; the peak near 890 km altitude is due principally to the January 2007 intentional destruction of the Fengyun-1C weather spacecraft while the peak centered at approximately 770 km altitude was created by the February 2009 accidental collision of Iridium 33 (active) and Cosmos 2251 (derelict) communication spacecraft [16,18]. The observations based on the incoherent scattering radar EISCAT ESR located at 78°N in Jul. 2006 and in Oct. 2015 [21,22,23] are respectively shown in Fig.7(c) and (d). This prediction to secondary peaks also agrees well with other space debris observations [24,25].

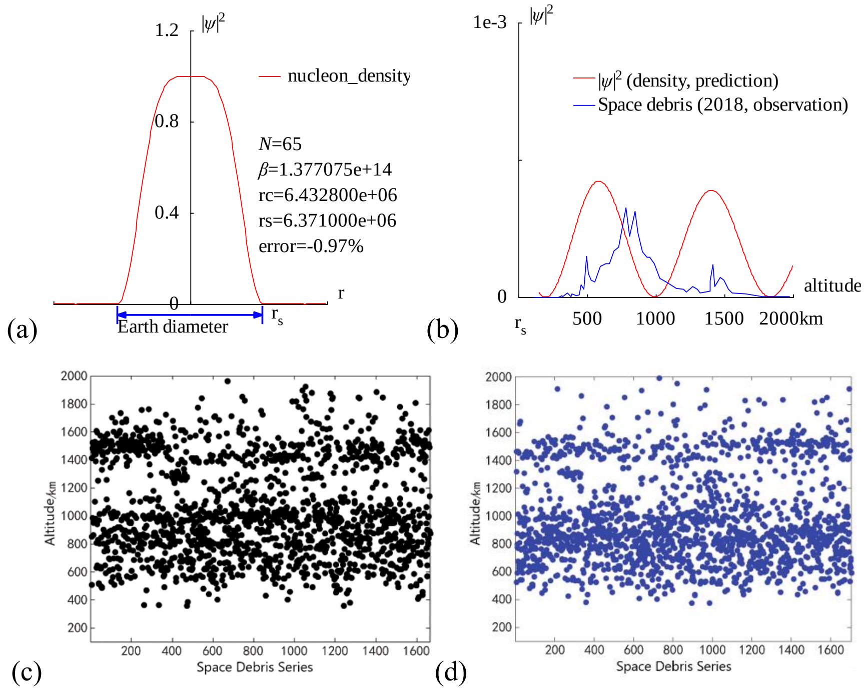

Fig.7 (a) The radius of the Earth is calculated out r=6.4328e+6 (m) with a relative error 0.97% by the interference of its acceleration-roll wave; (b) The prediction of the space debris distribution up to 2000km altitude; (c) The pace debris distribution in Jul. 2006, Joint observation based on the incoherent scattering radar EISCAT ESR located at 78°N [21]; (d) The space debris distribution in Oct. 2015, Joint observation based on the incoherent scattering radar EISCAT ESR located at 78°N [21].

```
<Clet2020 Script>//Clet v3 is a free C compiler[26]
int i,j,k,m,n,N,nP[10];
double H,B,M,v_r,r,AU,r_unit,x,y,z,delta,D[10],S[1000];
double rs,rc,rot,a,b,atm_height,beta; char str[100];
main(){k=80;rs=6.371e6;rc=0;atm_height=1.5e5;n=0; N=65;
beta=1.377075e+14;H=SPEEDC*SPEEDC*SPEEDC/beta;
M=5.97237e24;AU=1.496E11;r_unit=1e-6*AU;
rot=2*PI/(24*60*60);//angular speed of the Earth
for(i=-k;i<k;i+=1) {r=abs(i)*r_unit;
if(r<rs+atm_height) v_r=rot*r*r; else v_r=sqrt(GRAVITYC*M*r);//around the Earth
delta=2*PI* v_r/H; y=SumJob("SLIT_ADD,@N,@delta",D); y=y/(N*N);
if(y>1) y=1; S[n]=i;S[n+1]=y; if(i>0 && rc==0 && y<0.001) rc=r;    n+=2;}
SetAxis(X_AXIS,-k,0,k,"r; ; ; ;");SetAxis(Y_AXIS,0,0,1.2,"#if|ψ|#su2#t;0;0.4;0.8;1.2;");
DrawFrame(FRAME_SCALE,1,0xafffaf); x=50;z=100*(rs-rc)/rs;
SetPen(1,0xff0000);Polyline(k+k,S,k/2,1," nucleon_density");
r=rs/r_unit;y=-0.05;D[0]=-r;D[1]=y;D[2]=r;D[3]=y;
SetPen(2,0x0000ff); Draw("ARROW,3,2,XY,10,100,10,10,",D);
Format(str,"#ifN#t=%d#n#ifβ#t=%e#nrc=%e#nrs=%e#nerror=%.2f%",N,beta,rc,rs,z);
TextHang(k/2,0.7,0,str);TextHang(r+5,y/2,0,"r#sds#t");TextHang(-r,y+y,0,"Earth diameter");
}#v07=?>A
```

```
<Clet2020 Script>//Clet v3 is a free C compiler[26]
int i,j,k,m,n,N,nP[10]; double H,B,M,v_r,r,AU,r_unit,x,y,z,delta,D[10],S[10000];
double rs,rc,rot,a,b,atm_height,p,T,R1,R2,R3; char str[100];
int
Debris[96]={110,0,237,0,287,0,317,2,320,1,357,5,380,1,387,4,420,2,440,3,454,14,474,9,497,45,507,26,527,19,557,17,597,34,63
4,37,664,37,697,51,727,55,781,98,808,67,851,94,871,71,901,50,938,44,958,44,991,37,1028,21,1078,17,1148,10,1202,9,1225,6,
1268,12,1302,9,1325,5,1395,7,1395,18,1415,36,1429,12,1469,22,1499,19,1529,9,1559,5,1656,4,1779,1,1976,1,};
main(){k=80;rs=6.371e6;rc=0;atm_height=1.5e5;n=0; N=65;
H=1.956611e11;M=5.97237e24;AU=1.496E11;r_unit=1e4;
rot=2*PI/(24*60*60);//angular speed of the Earth
b=PI/(2*PI*rot*rs*rs/H); R1=rs/r_unit;R2=(rs+atm_height)/r_unit;R3=(rs+2e6)/r_unit;
for(i=R2;i<R3;i+=1) {r=abs(i)*r_unit; delta=2*PI*sqrt(GRAVITYC*M*r)/H;
y=SumJob("SLIT_ADD,@N,@delta",D); y=1e3*y/(N*N);// visualization scale:1000
if(y>1) y=1; S[n]=i;S[n+1]=y;n+=2;}
SetAxis(X_AXIS,R1,R1,R3,"altitude; r#sds#t;500;1000;1500;2000km ;");
SetAxis(Y_AXIS,0,0,1,"#if|ψ|#su2#t;0; ;1e-3;");DrawFrame(FRAME_SCALE,1,0xafffaf); x=R1+(R3-R1)/5;
```

```
SetPen(1,0xff0000);Polyline(n/2,S,x,0.8,"#if|ψ|#su2#t (density, prediction)");
for(i=0;i<48;i+=1) {S[i+i]=R1+(R3-R1)*Debris[i+i]/2000; S[i+i+1]=Debris[i+i+1]/300;}
SetPen(1,0x0000ff);Polyline(48,S,x,0.7,"Space debris (2018, observation) ");
}#v07=?>A
```

6. Mars and Jovian planets

The Mars and its satellites are quantized very well by its ultimate acceleration β as shown in Fig.8(a). Now let us talk about the Mars in the central state with quantum number n=0, its ultimate acceleration is β=2.581555e+15(m/s^2) in the Mars system. We have estimated the Mars overlapping number N=55 in Table 2, the matter distribution $|\psi|^2$ around the Mars can been calculated out in radius direction as shown in Fig.8(b), where the self-rotation at equator has the period of 24 hours.

The radius of the Mars is calculated out as r=1.6e+6 (m) with a relative error 52.79%, no further attempt was made to improve the calculation, because of limited knowledge about the Mars history. But one thing is certain, the Mars has frequently bombarded with smaller objects, in fact, consequently with the inclination of 25.2 degrees, so that its self-rotation is unstable or incorrect for its formation in a sense. At very beginning, the Mars self-rotation should have a period of 100 hours. Thanks to the Mars for safeguarding the Earth.

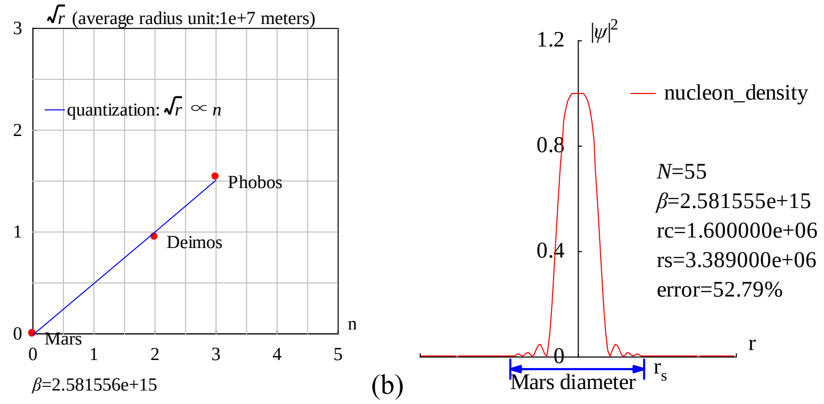

(a) (b)

Fig.8 (a)Quantization of Mars and its satellites. (b)The matter distribution $|\psi|^2$ around the Mars has been calculated in radius direction.

```
<Clet2020 Script>//Clet v3 is a free C compiler[26]
int i,j,k,m,n,N,nP[10];
double H,B,M,v_r,r,AU,r_unit,x,y,z,delta,D[10],S[1000],F[1000];
double rs,rc,rot,a,b,atm_height,beta; char str[100];
main(){k=80;rs=3.389e6;rc=0;atm_height=10e3;n=0; N=55;
beta=2.581555e+15; H=SPEEDC*SPEEDC*SPEEDC/beta;
M=0.107*5.97237e24; AU=1.496E11;r_unit=1e5;
rot=2*PI/(24*60*60);//angular speed
for(i=-k;i<k;i+=1) {r=abs(i)*r_unit;
if(r<rs+atm_height) v_r=rot*r*r; else v_r=sqrt(GRAVITYC*M*r);//around the star
delta=2*PI* v_r/H;y=SumJob("SLIT_ADD,@N,@delta",D); y=y/(N*N);
if(y>1) y=1; S[n]=i;S[n+1]=y; if(i>0 && rc==0 && y<0.001) rc=r;    n+=2;}
SetAxis(X_AXIS,-k,0,k,"r; ; ; ;");SetAxis(Y_AXIS,0,0,1.2,"#if|ψ|#su2#t;0;0.4;0.8;1.2;");
DrawFrame(FRAME_SCALE,1,0xafffaf); x=50;z=100*(rs-rc)/rs;
SetPen(1,0xff0000);Polyline(k+k,S,k/3,1," nucleon_density");
r=rs/r_unit;y=-0.05;D[0]=-r;D[1]=y;D[2]=r;D[3]=y;
SetPen(2,0x0000ff); Draw("ARROW,3,2,XY,10,100,10,10,",D);
Format(str,"#ifN#t=%d#n#ifβ#t=%e#nrc=%e#nrs=%e#nerror=%.2f%",N,beta,rc,rs,z);
TextHang(k/2,0.7,0,str);TextHang(r+5,y/2,0,"r#sds#t"); TextHang(-r,y+y,0,"Mars diameter");
}#v07=?>A
```

In order to extend the quantization rule to the Jovian planets (Jupiter, Saturn, Uranus and Neptune), it is necessary to further study the magnet-like components of gravity [28], the issue beyond the scope of this paper.

7. New aspect: coherent width and Sunspot cycle

It is common to mention **coherent length** of a wave, but one rarely talks about **coherent width** of a wave in quantum mechanics, simply because the latter is not a matter for electrons, nucleon or photos, but it is a matter in astrophysics. Analyzing observational data tells us that the coherent width of an acceleration-roll wave can extend to a 1000km or even more in planetary scale, as illustrated in Fig.9(a), the overlapping can even happen in width-direction bringing with a new aspect for wave interference.

In the solar convective zone, adjacent convective arrays form a top-layer flow, a middle-layer gas and a ground-layer reverse flow, (like the concept of **molecular current** in electromagnetism). Considering one convective ring at the equator as shown in Fig.9(b), there is an apparent velocity difference between the top-layer flow and the middle-layer gas, where their acceleration-roll waves are denoted respectively by

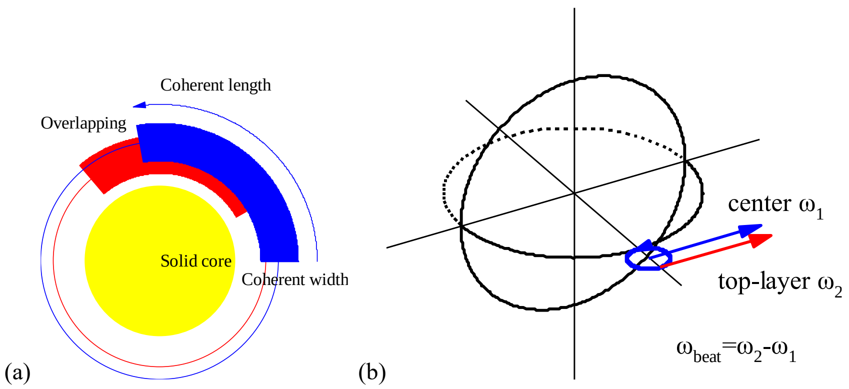

Fig.9 (a) Illustration of overlapping in coherent width direction. (b)One convective ring at the equator, the speed difference causes a beat frequency.

```
<Clet2020 Script>
int i, j, k, R,D[500];
main(){DrawFrame(FRAME_NULL,1,0xafffaf);
R=60; SetPen(1,0xffff00);
D[0]=-R; D[1]=-R; D[2]=R; D[3]=R; Draw("ELLIPSE,1,2,XY,0",D);
R=85;   k=15; SetPen(1,0xff0000);
D[0]=-R; D[1]=-R; D[2]=R; D[3]=R; Draw("ELLIPSE,0,2,XY,0",D);
D[0]=0; D[1]=0; D[2]=R-k; D[3]=0; D[4]=R+k;D[5]=0;
Draw("SECTOR,1,3,XY,15,30,130,0",D);
R=95; k=15; SetPen(1,0x00ff);
D[0]=-R; D[1]=-R; D[2]=R; D[3]=R; Draw("ELLIPSE,0,2,XY,0",D);
D[0]=0; D[1]=0; D[2]=R-k; D[3]=0; D[4]=R+k;D[5]=0;
Draw("SECTOR,1,3,XY,15,0,100,0",D);D[4]=R+k+k;
Draw("SECTOR,3,3,XY,15,0,100,0",D);
TextHang(0,0,0,"Solid core");TextHang(R-k-k,-k,0,"Coherent width");
TextHang(0,R+k+k+k,0,"Coherent length");TextHang(-R,R+k,0,"Overlapping");
}#v07=?>A
```

```
<Clet2020 Script>//Clet v3 is a free C compiler[26]
double beta,H,M,N,dP[20],D[2000],r,rs,rot,x,y,v1,v2,K1,K2,T1,T2,T,Lamda,V;
int main(){beta=2.961520e10; H=SPEEDC*SPEEDC*SPEEDC/beta;
M=1.9891E30; rs=6.95e8;rot=2*PI/(25.05*24*3600);v1=rot*rs;K1=v1*v1/2;//T1=2*PI*H/K1;
v2=0.7346*sqrt(BOLTZMANN*5700/MP)+0.2485*sqrt(BOLTZMANN*5700/(MP+MP));
K2=v2*v2/2;T2=2*PI*H/(K2-K1);T=T2/24*3600*365.2422;
Lamda=2*PI*H/(v2-v1);V=Lamda/T2;
SetViewAngle("temp0,theta60,phi-60");
DrawFrame(FRAME_LINE,1,0xafffaf);Overlook("2,1,60", D);
TextAt(10,10,"v1=%d, v2=%d, T=%.2f y, λ=%e, V=%d",v1,v2,T, Lamda,V);
TextJob("14","70,0,0,70,0,20,80,0,0,200,10,10,0",dP);Lattice(OVAL,dP,D);
SetPen(3,0x4f4fff);Plot("POLYLINE,4,200,XYZ,10",D[9]);
SetPen(2,0xff0000);Draw("ARROW,0,2,XYZ,15","80,0,0,80,60,0");
TextHang(100,20,0,"top-layer ω#sd2#t"); SetPen(2,0x0000ff);
Draw("ARROW,0,2,XYZ,15","70,0,0,70,60,0");
TextHang(40,60,0,"center ω#sd1#t");TextHang(140,-30,0," ω#sdbeat#t=ω#sd2#t-ω#sd1#t");
}#v07=?>A
```

$$\begin{aligned}\psi_{middle} &= \exp[\frac{i\beta}{c^3}\int_L (v_1 dl + \frac{-c^2}{\sqrt{1-v_1^{\ 2}/c^2}}dt)] \\ \psi_{top} &= \exp[\frac{i\beta}{c^3}\int_L (v_2 dl + \frac{-c^2}{\sqrt{1-v_2^{\ 2}/c^2}}dt)]\end{aligned} \quad . \tag{25}$$

Their overlapping wave interference in coherent width direction leads to a beat phenomenon

$$\begin{aligned}&|\psi|^2 = |\psi_{middle} + \psi_{top}|^2 = 2 + 2\cos[\frac{2\pi}{\lambda_{beat}}\int_L dl - \frac{2\pi}{T_{beat}}t] \\ &\frac{2\pi}{T_{beat}} = \frac{\beta}{c^3}(\frac{c^2}{\sqrt{1-v_2^{\ 2}/c^2}} - \frac{c^2}{\sqrt{1-v_1^{\ 2}/c^2}}) \simeq \frac{\beta}{c^3}(\frac{v_2^{\ 2}}{2} - \frac{v_1^{\ 2}}{2}) \\ &\frac{2\pi}{\lambda_{beat}} = \frac{\beta}{c^3}(v_2 - v_1); \quad V = \frac{\lambda_{beat}}{T_{beat}} = \frac{1}{2}(v_2 + v_1)\end{aligned} \quad . \tag{26}$$

Their speeds are calculated by

$$\begin{aligned}&v_1 = \omega r_{middle} = 2017\ (m/s) \quad \text{(sun rotation)}; \\ &v_2 \approx 6200\ (m/s) \quad (\approx \text{observed in Evershed flow})\end{aligned} \quad . \tag{27}$$

There are three ways to estimate the top-layer flow speed v_2. (1) regarding the Evershed flow as the eruption of the top-layer flow, about 6km/s speed was reported [31]. (2) regarding the prominences as the eruption of the top-layer flow; the prominence turbulent speeds are reported [31] in the range 2-10km/s. (3) Alternatively, since the thermal equilibrium gas in a convective zone supplies the flow speed v_2, where the temperature T=5700°K, the flow consists of 73.46% hydrogen atoms and 24.85% helium atoms; these atoms are approximately regarded as in 1D circular flow: $mv^2/2=kT/2$. Thus, the top-layer speed v_2 can be estimated out by

$$\begin{aligned}&v_2 \approx 0.7346\sqrt{\frac{kT}{m_{hydrogen}}} + 0.2485\sqrt{\frac{kT}{m_{helium}}} \\ &= 6244\ (m/s)\end{aligned} \quad . \tag{28}$$

Their beat period T_{beat} is calculated out to be a very remarkable value 10.38 (years), in agreement with the sunspot cycle value (say, mean 11years).

$$T_{beat} \simeq \frac{4\pi c^3}{\beta\left(v_2^{\ 2} - v_1^{\ 2}\right)} = 10.38\ (years) \ . \tag{29}$$

The relative error to the mean 11 years is 5.6% for the beat period calculation using the acceleration-roll waves. This beat turns out to be a density wave that undergoes to drive the sunspot cycle evolution. Comparing to the beat wavelength λ_{beat}, in order of magnitude, only the beat period is easy to be observed.

In the above calculation, although this seems to be a rough model, there is an obvious correlation between solar radius, solar rotation, solar density, ultimate acceleration and Planck-constant-like constant h.

8. Double slit interference: single particle algorithm

Consider a space shuttle with a couple of wings --- two huge solar energy panels as the wings, it flies within the space debris around the earth discussed in the preceding sections. The space debris passes through the two wing gaps between the shuttle body and the solar energy panels, they can be viewed as that situation like usual electron double-slit experiments, the space debris is regarded as the incident uniform particle beam to the space shuttle. Is there the inference phenomenon for the space debris behand the space shuttle? It is easy for astronaut's radar to observe this effect. But at present stage, we need to establish a calculation method which is suitable for describing the quantum behavior of single space debris.

Stemming from the double-slit electron interference algorithm [28], we first consider how to describe the quantum behavior of single electron. Consider two electrons q_1 and q_2, if the acceleration-roll of the particle q_1 (matter wave ϕ_1) overlaps with the acceleration-roll of the particle q_2 (matter wave ϕ_2), then we can calculate out the force acting on the particle q_1 by

$$\begin{aligned} &\psi = \phi_1 + \phi_2; \quad \mathbf{p} = \frac{1}{\psi\psi^*} \cdot \frac{\hbar}{2i}(\psi^*\nabla\psi - \psi\nabla\psi^*) \\ &f_x = \frac{d}{dx}\left(\frac{p^2}{2m} + U\right) \end{aligned} \quad . \tag{0.30}$$

where U is the potential energy. This force is called as the **adaptive force** with respect to the local ϕ_1 and ϕ_2, which guides the motion of the particles q_1 and q_2 like in the Newtonian mechanics; it is responsible for all quantum behaviors.

Using this physical thought, electron two slit interference was simulated, as shown in Fig.10 and Fig.11. The algorithm of the computer simulation for two slit interference runs within four steps: (1) When electrons pass through the slit 1, one by one, the matter wave is a cylinder matter wave ϕ_1 which occupies the whole space between the silts-plate and the screen. The electrons passed through the slit 2 have the similar cylinder matter wave ϕ_2. Both ϕ_1 and ϕ_2 have the same initial phase duo to the slit 0 as an initial filter. (2) An electron passes through the silt 1 with the momentum p, substituting ϕ_1 and ϕ_2 into the adaptive force formula, the adaptive force acting on the electron can be calculated out and be used to determine the next position of the particle like in the Newton mechanics, step by step, until the electron hits the screen. (3) Uniformly shooting electrons by the slit 1 to the screen, a bunch of electronic trajectories are got; repeating the calculation for the electrons passing through the slit 2, all hitting positions on the screen are recorded. (4) After many thousands of electrons are sent through the apparatus, fringes appear on the screen with a pattern.

The source code of the algorithm in C contains the detailed notes to help understand the transition process from Newton behaviors to quantum behaviors.

Fig.10 displays the distribution of 200 electron trajectories simulated using this algorithm, with a pattern that is exactly what we would expect for electron interference, like the Bohm trajectories for the two slit experiments, the tracks have kinks due to the adaptive force.

Fig.11 displays the hitting density distribution of 2000 electrons on the screen with a quantum interference pattern, in agreement with the prediction of Schrödinger and Bohm theories.

In this simulation, the adaptive force guiding the electron motion is produced by the superposition of matter waves ϕ_1 and ϕ_2.

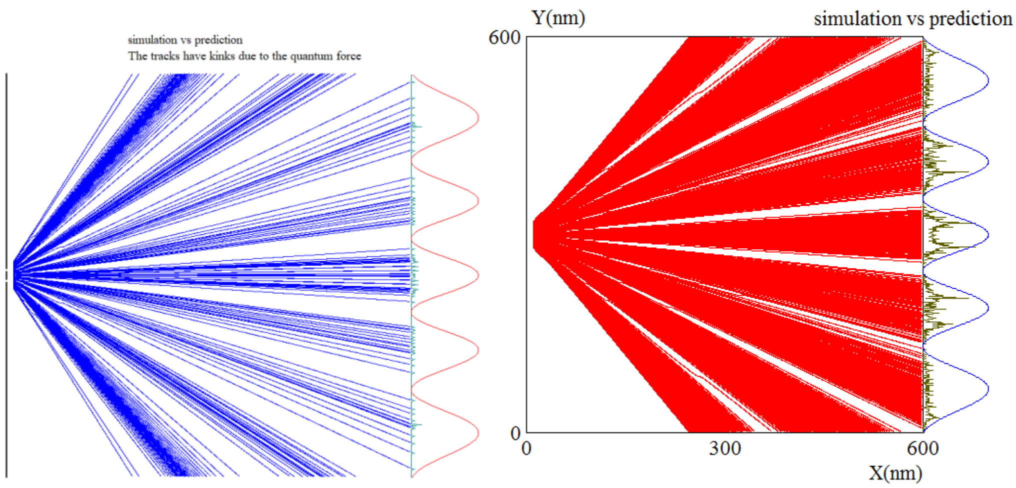

Fig.10 (a)200 trajectories, the kinks of the trajectories are due to the adaptive force. (b)Hitting density distribution of 2000 electrons on the screen.

Source Code: electron two slit interference

```
<Clet2020 Script>//Clet v3 is a free C compiler[26]
double x,y,z,vx,vy,Time_Step,N,Width,D[4000];//1D array
double r2,r3,r,x1,y1, phase;//variables
double L_unit,L,v0,p,Y,y01,y02,Y3,StartY,Density[600];int i,j,k; char Str[100];
double a,b,step,h,H,Z[10],Psi[10],Psi1[10],Psi2[10];;
main(){L_unit=1E-9;//1nm
Width=600;//width of screen
for(i=0;i<Width;i+=1) Density[i]=0;//clear
L=Width*L_unit;//size of window
v0=2E5;//initial speed,M/s
p=ME*v0/PLANCKBAR;//wave vector
H=PLANCKBAR/ME;
N=1000;Time_Step=L/(v0*N);y01=290*L_unit;//slit1 at (0,Y1)
y02=310*L_unit;//slit2 at (0,Y2)
Y3=(y02-y01);//the interval
SetAxis(X_AXIS,0,0,L,"X(nm);0;300;600;");SetAxis(Y_AXIS,0,0,L,"Y(nm);0;600;");
DrawFrame(FRAME_NULL,2,0xffffff);SetPen(2,0);
D[0]=0;D[1]=0;D[2]=0;D[3]=y01;Draw("LINE,0,2,XY",D);
D[0]=0;D[1]=y02;D[2]=0;D[3]=L;Draw("LINE,0,2,XY",D);
D[0]=0;D[1]=y01+Y3/5;D[2]=0;D[3]=y02-Y3/5;Draw("LINE,0,2,XY",D);
SetPen(1,0x0000ff);
for(StartY =-20; StartY <=20; StartY +=0.2){ x=10*L_unit;y=(Width/2+ StartY)*L_unit;//start point
 phase=0;   x1=0;y1=0;//displacement
 for(i=0;i<2000;i+=1)//get track
 {   D[i+i]=x; D[i+i+1]=y;
   Psi_Velocity();

   x1=vx*Time_Step; y1=vy*Time_Step; //advance one step
   phase+=ME*(vx*x1+vy*y1)/PLANCKBAR;   x+=x1; y+=y1;   if(y<0 || y>L ) break;//out
   if(x>L)   {k=y/L_unit;//transform for recording
     if(k>=0 && k<Width) Density[k]=Density[k]+1;//add one record
     break;   }
 }//hit on the screen
 Polyline(i,D);//track
}
for(i=0;i<Width;i+=1)//output data to clipboard
{y=i*L_unit; x=Density[i];   Format(Str,"y=%f, x=%f,",y,x);//theoretical prediction if you know
  ClipJob (APPEND,Str);//push these values to the clipboard.
}
for(i=0;i<Width;i+=1) { y=i*L_unit; x=L+Density[i]*5*L_unit;   D[i+i]=x;D[i+i+1]=y;}
SetPen(1,0x007f7f); Polyline(Width,D); //density
x1=PLANCKBAR/(ME*v0);//wavelength
for(i=0;i<Width;i+=1){   r=(i-290)*(i-290)+Width*Width;   r2=(i-310)*(i-310)+Width*Width;
  r=sqrt(r);r2=sqrt(r2);   r=(r2-r)*L_unit;   r=r/x1;   y=i*L_unit; x=L+(cos(r)+1)*50*L_unit;
  D[i+i]=x;D[i+i+1]=y;} SetPen(1,0xff0000); Polyline(Width,D);//intensity prediction
TextAt(380,150,"simulation vs prediction#nThe tracks have kinks due to the adaptive force");
}}

Psi_Value(){//known: x,y,w,r0;t;
r=sqrt(x*x+(y-y01)*(y-y01));b=v0*r/H;
Psi1[0]=cos(b)/r;Psi1[1]=sin(b)/r;Psi1[2]=1/r;
r=sqrt(x*x+(y-y02)*(y-y02));b=v0*r/H;
Psi2[0]=cos(b)/r;Psi2[1]=sin(b)/r;Psi2[2]=1/r;
Psi[0]=Psi1[0]+Psi2[0]; Psi[1]=Psi1[1]+Psi2[1]; Psi[2]=Psi[0]*Psi[0]+Psi[1]*Psi[1];}

Psi_Velocity(){ step=L_unit/1000000000;
Psi_Value();Z[0]=Psi[0];Z[1]=Psi[1];Z[2]=Psi[2];
```

```
h=x;x+=step;Psi_Value();x=h;
Complex(SUBTRACT,Psi,Z,Z[4]);Psi[1]=-Psi[1];Complex(MULTIPLY,Psi,Z[4],Z[6]);
vx=H*Z[7]/(step*Z[2]);
h=y;y+=step;Psi_Value();y=h;
Complex(SUBTRACT,Psi,Z,Z[4]);Psi[1]=-Psi[1];Complex(MULTIPLY,Psi,Z[4],Z[6]);
vy=H*Z[7]/(step*Z[2]);
}
#v07=?>A
```

In the future, we will apply this algorithm to study the quantum behavior of single space debris.

9. Conclusions

In analogy with the ultimate speed c, there is an ultimate acceleration β, nobody's acceleration can exceed this limit β, in the solar system, β=2.961520e+10(m/s^2). Because this ultimate acceleration is a large number, any effect connecting to β will become easy to test, including quantum gravity tests. In this paper, an approach is put forward to connect the ultimate acceleration with quantum theory, as an application, the quantum theory with the ultimate acceleration provides a useful formula to calculate the space debris distribution around the earth, this calculation results agree well with the experimental observation which are a set of measurements by incoherent scattering radar of EISCAT in the Arctic circle. Using the same approach, the radius of the Sun is calculated out to be r=7e+8 (m) with a relative error 0.72%; the radius of the Earth is calculated out to be r=6.4328e+6 (m) with a relative error 0.97%. The double-slit interference of space debris is also investigated for demonstrating its quantum behavior.

References

[1]C. Marletto, and V. Vedral, Gravitationally Induced Entanglement between Two Massive Particles is Sufficient Evidence of Quantum Effects in Gravity, Phys. Rev. Lett., 119, 240402 (2017)

[2]T. Guerreiro, Quantum effects in gravity waves, Classical and Quantum Gravity, 37 (2020) 155001 (13pp).

[3]S. Carlip, D. Chiou, W. Ni, R. Woodard, Quantum Gravity: A Brief History of Ideas and Some Prospects, International Journal of Modern Physics D, V,24,14,2015,1530028. DOI:10.1142/S0218271815300281.

[4]de Broglie, L., CRAS,175(1922):811-813, translated in 2012 by H. C. Shen in Selected works of de Broglie.

[5]de Broglie, Waves and quanta, Nature, 112, 2815(1923): 540.

[6]de Broglie, Recherches sur la théorie des Quanta, translated in 2004 by A. F. Kracklauer as De Broglie, Louis, On the Theory of Quanta. 1925.

[7]NASA, https://solarscience.msfc.nasa.gov/interior.shtml.

[8]NASA, https://nssdc.gsfc.nasa.gov/planetary/factsheet/marsfact.html.

[9]B. Ryden Introduction to Cosmology, Cambridge University Press, 2019, 2nd edition.

[10]D. Valencia, D. D. Sasselov,R. J. O'Connell, Radius and structure models of the first super-earth planet, The Astrophysical Journal, 656:545-551, 2007, February 10.

[11]D. Valencia, D. D. Sasselov,R. J. O'Connell, Detailed models of super-earths: how well can we infer bulk properties? The Astrophysical Journal, 665:1413–1420, 2007 August 20.

[12]T. Guillot, A. P. Showman, Evolution of "51Pegasusb-like" planets, Astronomy & Astrophysics,2002, 385,156-165, DOI: 10.1051/0004-6361:20011624

[13]T. Guillot, A. P. Showman, Atmospheric circulation and tides of "51Pegasusb-like" planets, Astronomy & Astrophysics,2002, 385,166-180, DOI: 10.1051/0004-6361:20020101

[14]L.N. Fletcher,Y.Kaspi,T. Guillot, A.P. Showman, How Well Do We Understand the Belt/Zone Circulation of Giant Planet Atmospheres? Space Sci Rev, 2020,216:30. https://doi.org/10.1007/s11214-019-0631-9

[15]Y. Kaspi, E. Galanti, A.P. Showman, D. J. Stevenson, T. Guillot, L. Iess, S.J. Bolton, Comparison of the Deep Atmospheric Dynamics of Jupiter and Saturn in Light of the Juno and Cassini Gravity Measurements,Space Sci Rev, 2020, 216:84. https://doi.org/10.1007/s11214-020-00705-7

[16]Orbital Debris Program Office, HISTORY OF ON-ORBIT SATELLITE FRAGMENTATIONS, National Aeronautics and Space Administration, 2018, 15 th Edition.

[17]M. Mulrooney, The NASA Liquid Mirror Telescope, Orbital Debris Quarterly News, 2007, April,v11i2,

[18]Orbital Debris Program Office, Chinese Anti-satellite Test Creates Most Severe Orbital Debris Cloud in History, Orbital Debris Quarterly News, 2007, April,v11i2,

[19]A. MANIS, M. MATNEY, A.VAVRIN, D. GATES, J. SEAGO, P. ANZ-MEADOR, Comparison of the NASA ORDEM 3.1 and ESA MASTER-8 Models, Orbital Debris Quarterly News, 2021, Sept,v25i3.

[20]D. Wright, Space debris, Physics today,2007,10,35-40.

[21]TANG Zhi-mei, DING Zong-hua, DAI Lian-dong, WU Jian, XU Zheng-wen, "The Statistics Analysis of Space Debris in Beam Parking Model in 78° North Latitude Regions," Space Debris Research, 2017, 17,3, 1-7.

[22]TANG Zhimei DlNG, Zonghua, YANG Song, DAI Liandong, XU Zhengwen, WU Jian The statistics analysis 0f space debris in beam parking model based On the Arctic 500 MHz incoherent scattering radar, CHINESE JOURNAL 0F RADIO SCIENCE, 2018, 25,5, 537-542

[23]TANG Zhimei， DING, Zonghua， DAI Liandong， WU Jian， XU Zhengwen, Comparative analysis of space debris gaze detection based on the two incoherent scattering radars located at 69N and 78N, Chin ．J ．Space Sci, 2018 38,1, 73-78. DOI:10.11728/cjss2018.01.073

[24]DING Zong-hua, YANG Song, JIANG hai, DAI Lian-dong, TANG Zhi-mei, XU Zheng-wen, WU Jian, The Data Analysis of the Space Debris Observation by the Qujing Incoherent Scatter Radar, Space Debris Research, 2018, 18,1, 12-19.

[25]YANG Song, DING Zonghua, Xu Zhengwe, WU Jian, Statistical analysis on the space posture, distribution, and scattering characteristic of debris by incoherent scattering radar in Qujing, Chinese Journal of Radio science, 2018 33,6 648-654, DOI:10.13443/j.cjors.2017112301

[26]Clet Lab, Clet: a C compiler, https://drive.google.com/file/d/1OjKqANcgZ-9V5 6rgcoMtOu9w4rP49sgN/view?usp=sharing

[27]Huaiyang Cui, Relativistic Matter Wave and Its Explanation to Superconductivity: Based on the Equality Principle, Modern Physics, 10,3(2020)35-52. https://doi.org/10.12677/MP.2020.103005

[28]Huaiyang Cui, Relativistic Matter Wave and Quantum Computer, Kindle ebook, 2021.

[29]Huaiyang Cui, Evidence of Planck-Constant-Like Constant in Five Planetary Systems and Its Significances, viXra:2204.0133, 2022.

[30]Huaiyang Cui, Approach to enhance quantum gravity effects by ultimate acceleration, viXra:2205.0053, 2022.

[31]N.Cox, Allen's Astrophysical Quantities, Springer-Verlag, 2001, 4th ed..